BioGecko

Vol 12 Issue 03 2023
ISSN NO: 2230-5807

ESTIMATION OF FLEXURAL STRENGTH ASSESSMENT OF ULTRA-HIGH STRENGTH CONCRETE USING ARTIFICIAL INTELLIGENCE

Dr Manik Deshmukh[1], Dr.S. Thenmozhi[2], Siddharth Jain[3], D. Gouse Peera[4], Amruta Jagdish Killol[5]
[1]Associate professor, SVERI'scollege of engineering Pandharpur, Email: mgdeshmukh@coe.sveri.ac.in
[2]Associate Professor, Civil Engineering,St.Joseph's College of Engineering, OMR, Chennai 600 119.
[3]Assistant Professor, Civil Engineering, KIET Group of Institutions,Delhi NCR, India
[4]Assistant Professor, Civil Engineering, Annamacharya Institute of Technology and Sciences, Rajampet, Andhra Pradesh, India 516126, Email:gouse_mgr@yhoo.in
[5]Assistant professor, Civil Engineering,Ajeenkya D.Y.Patil School of Engineering, Lohgaon, Pune, Email Id: killolamruta9@gmail.com

Abstract: The development of novel approaches, such as supervised machine learning algorithms that can quickly determine the mechanical characteristics of fiber-reinforced concrete, has been the focus of research. The objective of this study is to predict the flexural strength (FS) of steel fiber-reinforced concrete (SFRC) utilising computational techniques necessary for efficient and rapid examination. To do this, a database containing the SFRC flexural data was compiled from literature research. To forecast the 28-day flexural strength of steel fiber-reinforced concrete, three ensembled models using machine learning techniques—Gradient Boosting (GB), Random Forest (RF), and Extreme Gradient Boosting (XGB)—were taken into consideration. Utilising the coefficient of determination (R2), statistical analysis, and k-fold cross-validation, the effectiveness of each approach was evaluated. To examine how different variables affected the ability to anticipate outcomes, a sensitivity method was also applied. According to the investigation, the GB and RF models performed admirably, and the XGB method was within acceptable bounds. With an R2 of 0.96, Gradient Boosting outperformed Extreme Gradient Boosting (XGB) and Random Forest (RF), which had R2 values of 0.94 and 0.86, respectively. Additionally, based on lowered error levels, statistical and k-fold cross-validation tests supported that Gradient Boosting was the top performance, followed by Random Forest (RF). Performance of the Extreme Gradient Boosting model was good. These ensemble machine learning techniques, especially for fiber-reinforced concrete, can help the construction industry by delivering quick and improved analyses of material characteristics.

Keywords: Concrete; steel fibre; concrete reinforced with steel fibre; flexural strength; mechanical properties; building materials

1 Introduction

According to earlier works of literature [1-6], the addition of steel fibres to concrete enhances its mechanical properties, including compressive strength, flexural strength, and tensile strength. This makes the concrete harder and more resistant to cracking. Flexural strength was much higher in steel fiber-reinforced concrete than in unreinforced concrete [7]. Investigations on the flexural behaviour of SFRC beams revealed that adding more steel fibre enhanced strength, toughness, and load-bearing capacity [8]. Concrete's lifespan and resistance to freezing were both improved by the inclusion of up to 15% steel fibres [9]. In terms of fibre volume fraction and curing time, the FS of SFRC was examined. It was shown that SFRC flexural toughness requires high-performance steel fibre and a high fibre volume percentage. Experimental research on the effects of fibre content and concrete strength on SFRC flexural behaviour was conducted [11].High-strength SFRC's toughness was increased by adding steel fibre and silica fume [12]. The flexural response of SFRC beams was studied analytically, and experimental findings were presented. The results showed that the increased steel fibre volume improved post-peak ductility, deflection capacity, and flexural strength [13]. Concerning the amount of steel fibres and the coarseness of the particle size, the mechanical properties of high-strength concrete were investigated. The findings

demonstrated that increasing the fibre content significantly raised the compressive and flexural toughness of the SFRC [14].

Recently developed machine learning (ML) algorithms are essential to the civil engineering sector because they can accurately anticipate the mechanical properties of concrete. Data analysis is carried out using machine learning (ML), a field of computer science that automates the development of analytical models. Algorithms for machine learning are created to learn from previously gathered data. Because it can handle a variety of different types and sizes of data, ML has become more and more popular. The computer process is also more efficient and less expensive. As a result, models for analysing large and complex data sets as well as for producing quicker and more accurate findings may be easily and automatically constructed.The use of these models yields extremely accurate predictions, enabling more skillful decisions and intelligent actions to be taken in real-time without requiring human interaction [26]. To reduce material and experimentation cycle waste, ML models to estimate concrete strength are currently being developed. One of the most cutting-edge modelling strategies utilised in civil engineering is artificial intelligence (AI) methodology, namely machine learning (ML).

These methods model reactions using input variables. Researchers have recently concentrated on the compressive strength of concrete as well as other strength features including flexural strength, tensile strength, and concrete durability using supervised machine learning approaches.Behnood et al. investigated the compressive, flexural, and split tensile strengths of concrete using the M5P model [27].

2. Data Description

The dataset was specifically produced using information from concrete with hook-end steel fibres.17 sources were used to get the data [8,11-14]. The outcomes that had a substantial influence on the criteria were chosen and processed. As a result, there are 10 different pieces in the dataset, comprising input and output data. These ten factors—each of which has an impact on SFRC flexural strength—were taken into consideration when estimating SFRC flexural strength.

2.1 Water and Cement

Prior studies have shown that concrete strength is strongly influenced by the water-to-cement ratio. Flexural strength and compressive strength are said to diminish when the water-cement ratio rises, according to Abbass et al. 29]. The flexural and compressive strengths of self-consolidating concrete were significantly impacted by the water-cement ratio, according to Reddy et al. [30]. Nili et al. proved through scientific research that SFRC achieved superior flexural strength with a lower water-cement ratio [31]. Using various cement doses and water-cement ratios, Merve A. Ikgen et al. studied the link between SFRC splitting tensile and flexural strength [32]. Wei Li looked into how the water-cement ratio affected the performance of concrete and found that when the ratio increases, the strength of the concrete decreases [33].Experimental research by M. S. Ahmad Shah et al. on the flexural strength of concrete at different water-cement ratios came to the conclusion that the flexural strength increased with increasing water-cement proportion [34]. Chang Joon Lee et al. investigated the effects of fibre content and the water-cement ratio on the flexural toughness of SFRC. A quicker flexural toughness convergence rate is produced by a lower water-cement ratio and a greater fibre volume [35]. E. K. Z. Balanji looked into the effects of steel fibre content and varied water-cement ratios on the mechanical properties and impact resistance of steel fibre concrete. When the water-cement ratio was smaller, steel fibres had a greater positive impact on mechanical properties and impact resistance [36].

2.2. Sand and Aggregate

A significant component has been identified as the effect of sand and aggregate fraction on the strength characteristics of SFRC. Kim et al. discovered that the SFRC's compressive and flexural strengths were increased by the larger sand to aggregate ratio [37]. According to Chitlange et al. [38], there was a significant difference in the flexural and compressive strength of concrete depending on the quantities of sand and aggregate employed. A comparison study of the flexural strength of concrete with various aggregate volumes and types was conducted by K. B. Dashrath et al. [39]. El-Ariss investigated the effects of the water-cement ratio, sand content, and curing procedure on the strength of concrete [40]. U.

M. Tarek and others.found the appropriate sand-aggregate ratio by analysing the impact of various sand-aggregate ratios on concrete strength parameters [41]. M. Sunarso and coworkers did researchsand-aggregate percentage and additive dosage effects on a variety of high-strength concrete properties [42]. Due to its significance in the concrete's strength characteristics, the sand to aggregate ratio was taken into consideration when designing the ML models.

2.3. Superplasticizer

A superplasticizer is a chemical that reduces the amount of water in concrete, which increases the strength of the final product. M. Khan and M. Ali [44] used superplasticizer and pozzolanic additives to enhance the mechanical qualities of concrete. Increased superplasticizer concentration improved the slump and strength characteristics of concrete, according to Aruntas et al. [45]. As a result, a superplasticizer was incorporated into the ML models to see how it would affect the SFRC's flexural strength.

2.4. Silica Fume

In different amounts, silica fume has been used to enhance the concrete's strength properties. According to Köksal et al., the addition of more silica fume increased the compressive and flexural strength of concrete [12]. According to M. Nili and V. Afroughsabet [25], the combined use of steel fibres and silica fume significantly increased the concrete's flexural strength. Concrete's flexural strength can be increased by 15% by replacing up to 7.5% of the cement with silica fume, according to M. Shafieyzadeh [41].According to M. Shmlls et al., silica fume and fly ash dose together improved the strength characteristics of concrete [42]. One factor that affects the strength properties of SFRC was found to be the silica fume inclusion.

2.5. Fly Ash

Both the workability of flexible concrete and the strength characteristics of hardened concrete are improved by fly ash. Fly ash was added to SFRC, and R. M. K. Saravana and A. Sumathi found that this increased the concrete's strength over time [44]. The impact of fly ash and steel fibres on the durability of pozzolana cement concrete was examined by M. A. Challoob et al. [44]. A.K. Saha discovered that the addition of fly ash progressively enhanced the concrete's strength [46]. Fly ash was partially added to high-strength concrete, according to P. Nath and P. Sarker, which increased its durability properties [47]. Fly ash was chosen as a variable as a result because of its connection to specific attributes.

2.6. Steel Fiber Volume, Length and Diameter

According to the literature, the percentage, length, and thickness of the steel fibres significantly affect the flexural strength of concrete. According to Yazici et al., adding more steel fibre to concrete boosted its compressive and flexural strength [7]. According to Köksal et al.'s experimental examination using fibre volume fractions up to 1% [12], SFRC compressive and flexural strength increased. According to A. A. Jhatial et al., the increasing steel fibre content enhanced the flexural and compressive strength [48]. Steel fibres in concrete significantly improved the strength and endurance of hardened concrete, according to research by H. K. Hussain et al. The addition of steel fibres with hooked ends greatly enhanced the flexural strength [49].

	Mean	Standard Error	Median	Mode	Range	Minimum	Maximum	Count
Cement (kg/m^3)	451.78	8.37	400	400	509	280	789	173
Water (kg/m^3)	170.66	2.29	158	152	137	133	270	173
Sand (kg/m^3)	782.75	11.47	740	835	768	582	1350	173
Coarse Aggregate (kg/m^3)	927.09	20.63	1050.5	1047	1170	0	1170	173
Superplasticizer (%)	0.91	0.13	0.15	0	5	0	5	173
Silica fume (%)	6.33	0.89	0	0	43	0	43	173

Fly Ash (%)	1.30	0.42	0	0	30	0	30	173
Volume fraction of the hooked steel fiber (%)	0.85	0.05	1	0.5	2	0	2	173
Fiber Length (mm)	40.41	1.21	35	60	60	0	60	173
Fiber diameter (mm)	0.59	0.01	0.615	0.75	0.9	0	0.9	173
Flexural Strength; MPa (28 days)	10.04	0.63	7.82	0	41.7	0	41.7	173

3. Research Strategy

The machine learning models were created using python code and anaconda software. Programmes that provide direction through Conda packages, channels, and environments can run using the Anaconda navigator, a graphical user interface that is part of the Anaconda software, without the need for command-line expertise. Additionally, it offers Python and R programming languages with an emphasis on package development and maintenance for use in data science and machine learning applications. Gradient Boosting (GB), Random Forest (RF), and Extreme Gradient Boosting (XGB) were employed in this study to predict the flexural strength of the SFRC. For model execution, the Anaconda navigator's Spyder (version: 4.3.5) was utilised. To assess the level of accuracy, the R2 value of each model's expected result was employed.

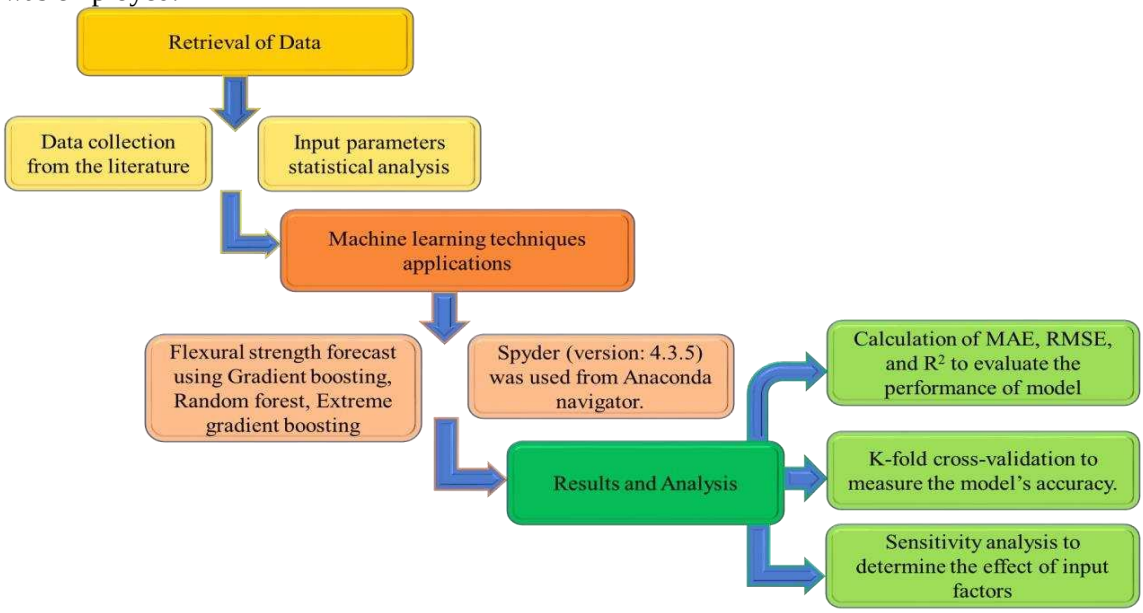

Figure 2. Methodology of research in order.

4. Results and Discussions

4.1. Statistical Analysis Explanation

Figure 3 displays a statistical trend comparing the actual and projected SFRC flexural strength after 28 days using the R-F model. The R-F generates outcomes that fall within the permitted range and have a minimal difference between expected and actual results. The model's ability to estimate outcomes is demonstrated by its R 2 value of 0.94. Figure 4 shows the R-F model's deviations as well as the distribution of actual and anticipated results. The distribution's maximum, minimum, and average error values were, in order, 7.09, 0.036, and 1.50 MPa. It was discovered that 52% of the inaccurate readings fell below 1 MPa, 44% fell between the range of 1 to 5, and 3.8% fell over 5 MPa. These data show how

closely predicted and actual results match up.5 MPa. These statistics indicate the degree of agreement between expected and actual results.

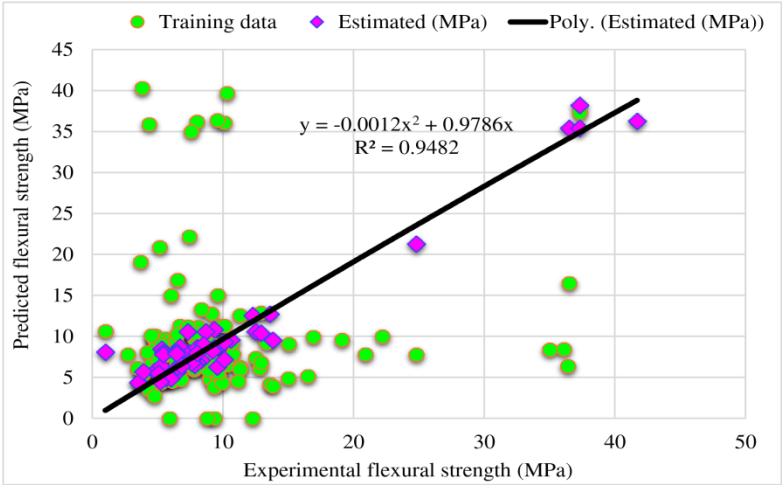

Figure 3. Relationship for R-F model: Experimental and estimated results.

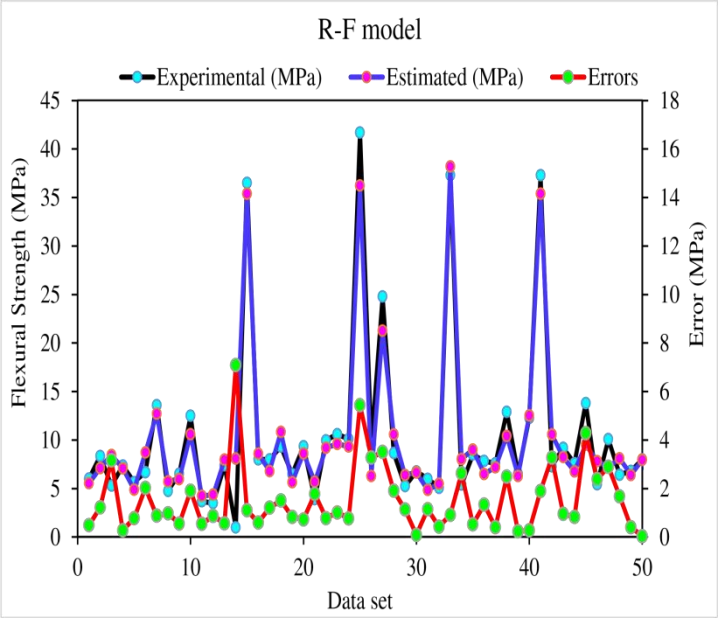

Figure 4. Experimental, estimated and, error values for R-F model.

Figures 5 and 6 show the results of the G-B model. Figure 5 depicts the link between actual and anticipated results. R2 = 0.96, which is greater than that of the R-F model, demonstrates that the G-B strategy works better than the R-F model. Figure 6 shows the distribution of actual and projected values, as well as errors, in the G-B model. Maximum, lowest, and average error values for the distribution were 5.4, 0.0026, and 1.34 MPa, respectively. The results showed that 42% of inaccurate readings were below 1 MPa, 56% were in the range of 1 to 5 MPa, and 2% were over 5 MPa. The SFRC flexural strength can be predicted more precisely by the G-B model based on the R2 and error distribution of the R-F and G-B models.

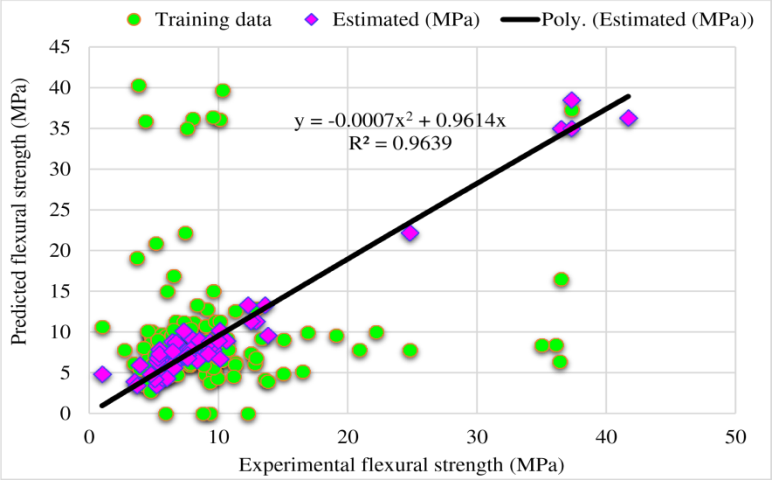

Figure 5. Experimental and estimated results connection for G-B model.

The link between the XGB model's actual and expected results is shown in Figure 7. The XGB model has an R2 value of 0.86, which indicates that it is less accurate than the R-F and G-B models. The distribution of errors and the actual and predicted values for the XGB model are also shown in Figure 8. The largest, lowest, and mean errors, in that order, were 8.88, 0.036, and 2.43 MPa. The results showed that 12% of the incorrect readings exceeded 5 MPa, 58% were between 1 MPa and 5 MPa, and 30% were less than 1 MPa. The G-B model was more accurate than the R-F and XGB models in this investigation as a result of decreased inaccuracy and greater R2 values.

4.2. Cross-Validation Using K Fold

The model's validity is checked during execution using the k-fold cross-validation method. The accuracy of a model with a dispersed and divided data set into 10 groups is typically checked using this technique [94–96]. With one group, the model was tested, and the other nine were trained. In all, 70% of the data set was utilised for model training, while the final 30% was used to assess the models.

The collection of observations must be randomly divided into k groups or folds that are approximately the same size. The subsequent k-1 folds are utilised to fit the process while the initial fold serves as a validation set.If the R2 value is high and the errors, such as MAE and RMSE, are small, the model is seen to be more accurate. To get a good outcome, you must repeat the method ten times. The model's great accuracy depends on this thorough approach. Additionally, all models were statistically analysed as errors (MSE and RMSE), as shown in Table 2. Equations (1) and (2) from the literature were employed in statistical analysis to evaluate how the models responded to estimate [97].

$$MAE = \frac{1}{n}\sum_{i=1}^{n}|x_i - x| \quad (1)$$

$$RMSE = \sqrt{\sum \frac{\left(y_{pred} - y_{ref}\right)^2}{n}} \quad (2)$$

where n = total number of sampled data. x, y_{ref} = reference values of data sample. x_i, y_{pred} = model-predicted values.

Table 2. Statistical analysis of the approaches used.

Models	MAE (MPa)	RMSE (MPa)	R2
Random Forest	1.5	2.0	0.94
Gradient Boosting	1.3	1.8	0.96
XGBoost	2.4	3.3	0.86

In Figures 9 through 11, you can see the MAE, RMSE, and R2 distributions for the k-fold cross-validation of the Random Forest, Gradient Boosting, and Extreme Gradient Boosting models. Figure 9 displays the greatest, lowest, and average R2 values for the R-F model, which are 0.94, 0.34, and 0.69, respectively. As shown in Figure 10, the highest, minimum, and average R2 values for the G-B model are 0.96, 0.33, and 0.74, respectively. The greatest, lowest, and average R2 values for the XGB are displayed in Figure 11, and they are 0.86, 0.36, and 0.64, respectively.When the error values were compared, the average MAE and RMSE for the R-F model were 2.94 and 4.58, respectively.

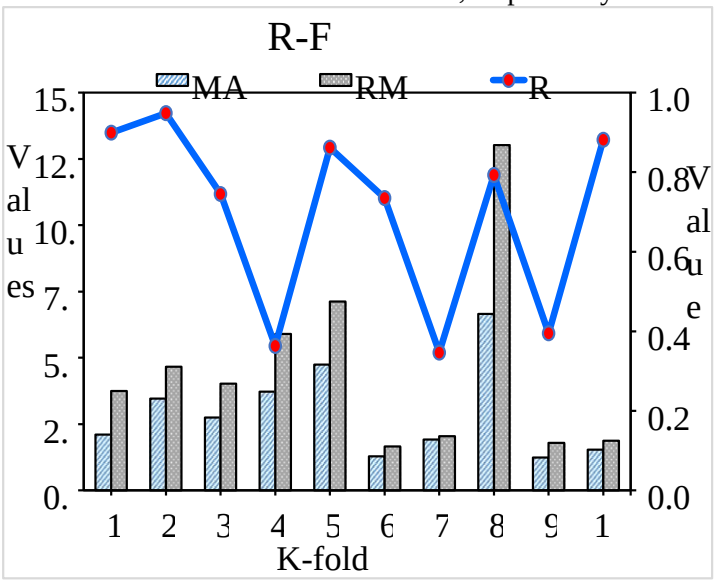

Figure 9. Random Forest model with K-fold cross-validation representation.

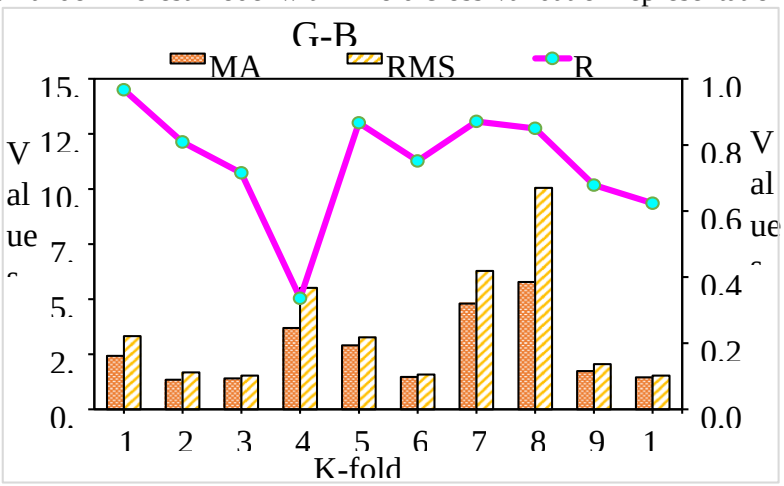

Figure 10. K-fold cross-validation representation for the Gradient Boosting model.

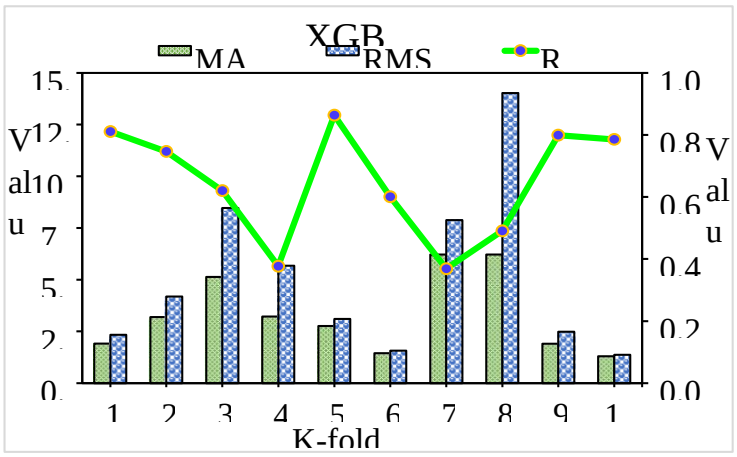

Figure 11. K-fold cross-validation representation for Extreme Gradient Boosting model.

4.3. Sensitivity Analysis

The purpose of this study is to determine how input factors affect SFRC flexural strength prediction. Figure 12 illustrates how input parameters affected the SFRC's forecast of flexural strength. Silica fume, which made up 21.7% of the total, was found to be the most important component, followed by cement (15.8%) and superplasticizer (6.4%). The remaining input factors, including sand (5.6%), water (11.2%), and coarse aggregate (8%), had a less significant impact on the flexural strength of the SFRC prediction. Impacts of steel fibre vf, fibre length, and fibre diameter were respectively 19.7%, 9.6%, and 2%. The results of the sensitivity analysis correlated with the amount of input parameters and data points used in the model design.

$$Ni = fmax(xi) - fmin(xi) \quad (3)$$

The highest and lowest projected outputs over the i^{th} output are represented by $f_{max}(x_i)$ and $f_{min}(x_i)$, respectively.

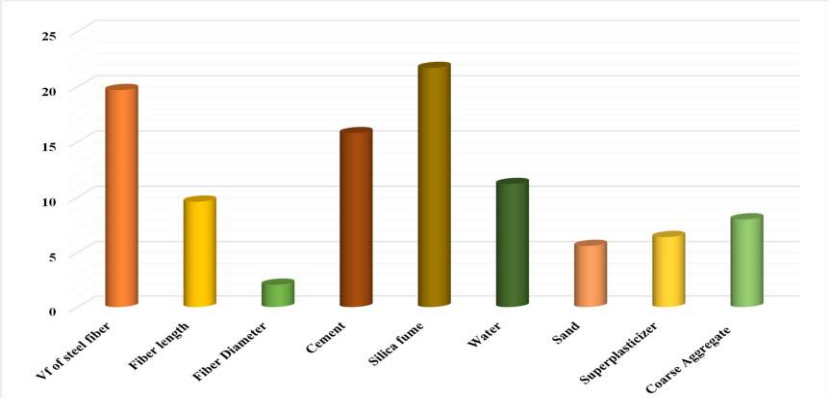

Figure 12. The input variable's contribution to the forecast.

5. Discussions

This study's objective was to ascertain whether SFRC flexural strength could be predicted using machine learning techniques. Three machine learning techniques were looked at: Extreme Gradient Boosting, Gradient Boosting, and Random Forest. The effectiveness of each technique was evaluated and compared in order to ascertain which one makes the most accurate predictions. With an R2 score of 0.96, the G-B model delivered a result that was more accurate. R2 was 0.81 and 0.87 for the R-F and XGB models, respectively. All models' efficacy was verified using statistical analysis and the k-fold cross-validation method. With fewer errors, the model performs better.The vulnerable intern is widely exploited by ML

approaches, which build sub-models that are maximised and trained on data to increase the value of R2. Figures 13–15 display the fluctuation in R2 values for several sub-models, including Random Forest, Gradient Boosting, and Extreme Gradient Boosting approaches. The highest, lowest, and mean R2 values for the Random Forest sub-model were 0.94, 0.34, and 0.69, respectively. The highest, minimum, and average R2 values for the Gradient Boosting (G-B) sub-models were 0.96, 0.63, and 0.79, respectively. For the Extreme Gradient Boosting sub-models, the highest, lowest, and mean R2 values were 0.87, 0.44, and 0.68, respectively. These findings show that the G-B sub-model outperforms the R-F and XGB sub-models in terms of accuracy.

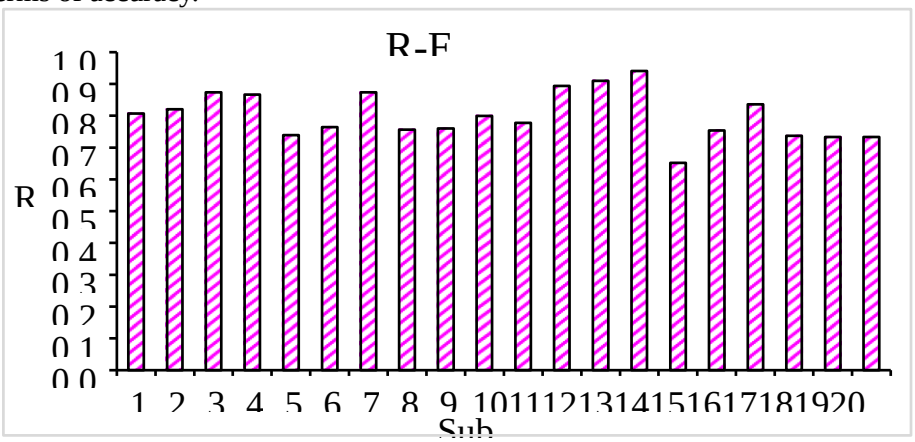

Figure 13. The coefficient correlation (R^2) values of the R-F sub-model.

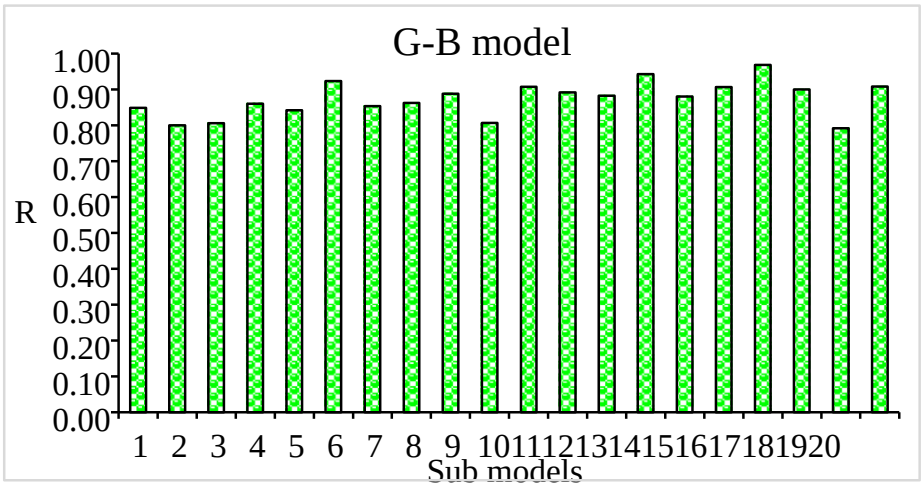

Figure 14. G-B sub-model's coefficient correlation (R^2) values.

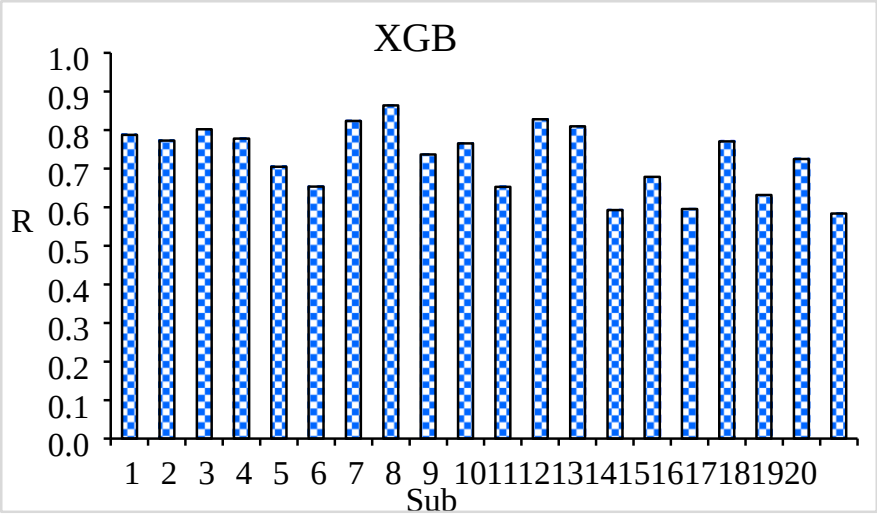

Figure 15. XGB sub-model's coefficient correlation (R^2) values.

6. Conclusion

This study sought to estimate the 28-day SFRC flexural strength using three ensembled ML algorithms. To predict the results, models for Random Forest (R-F), Gradient Boosting (G-B), and Extreme Gradient Boosting (XGB) were used. The findings of this research are:

1) When projecting SFRC flexural strength, the Extreme Gradient Boosting (XGB) model performed worse than the Gradient Boosting (G-B) and Random Forest (R-F) models.

2) In terms of predicting the 28-day flexural strength of SFRC, the Gradient Boosting model performed better than the Extreme Gradient Boosting and Random Forest ensemble machine learning techniques.

3) The coefficients of determination (R2) for the Random Forest, Gradient Boosting, and Extreme Gradient Boosting models are 0.94, 0.96, and 0.86, respectively. Although there is a small deviation from the precise results, all of the model outputs are within acceptable ranges.

4) The Gradient Boosting model fared better than the other models analysed in terms of prediction, as shown by the k-fold cross-validation test and statistical analysis.

5) In order to establish how much the input parameters mattered, a sensitivity analysis was performed. It was found that the prediction of the outcome depended on the following variables: Vf of steel fibre, Fibre length, Fibre diameter, Cement, Silica fume, Water, Sand, Superplasticizer, and Coarse Aggregate, respectively.

6) Without the need for extensive casting and testing, the ensemble machine learning algorithms, particularly Gradient Boosting, can accurately estimate the strength properties of concrete.

References

1. Khan, M.; Cao, M.; Xie, C.; Ali, M. Effectiveness of hybrid steel-basalt fiber reinforced concrete under compression. *Case Stud. Constr. Mater.* **2022**, *16*, e00941. [CrossRef]
2. Khan, M.; Cao, M.; Chu, S.; Ali, M. Properties of hybrid steel-basalt fiber reinforced concrete exposed to different surrounding conditions. *Constr. Build. Mater.* **2022**, *322*, 126340. [CrossRef]
3. Cao, M.; Xie, C.; Li, L.; Khan, M. The relationship between reinforcing index and flexural parameters of new hybrid fiber reinforced slab. *Comput. Concr.* **2018**, *22*, 481–492. [CrossRef]
4. Cao, M.; Khan, M. Effectiveness of multiscale hybrid fiber reinforced cementitious composites under single degree of freedom hydraulic shaking table. *Struct. Concr.* **2020**, *22*, 535–549. [CrossRef]

5. Ali, B.; Kurda, R.; Ahmed, H.; Alyousef, R. Effect of recycled tyre steel fiber on flexural toughness, residual strength, and chloride permeability of high-performance concrete (HPC). *J. Sustain. Cem. Mater.* **2022**, 1–17. [CrossRef]
6. Ali, B. Development of environment-friendly and ductile recycled aggregate concrete through synergetic use of hybrid fibers. *Environ. Sci. Pollut. Res.* **2022**, *29*, 34452–34463. [CrossRef] [PubMed]
7. Yazıcı, G.; Inan, G.; Tabak, V. Effect of aspect ratio and volume fraction of steel fiber on the mechanical properties of SFRC. *Constr. Build. Mater.* **2007**, *21*, 1250–1253. [CrossRef]
8. Yoo, D.-Y.; Yoon, Y.-S.; Banthia, N. Flexural response of steel-fiber-reinforced concrete beams: Effects of strength, fiber content, and strain-rate. *Cem. Concr. Compos.* **2015**, *64*, 84–92. [CrossRef]
9. Nili, M.; Azarioon, A.; Danesh, A.; Deihimi, A. Experimental study and modeling of fiber volume effects on frost resistance of fiber reinforced concrete. *Int. J. Civ. Eng.* **2016**, *16*, 263–272. [CrossRef]
10. Jang, S.; Yun, H. Effects of Curing Age and Fiber Volume Fraction on Flexural Behavior of High-Strength Steel Fiber-Reinforced Concrete. *J. Korean Soc. Hazard Mitig.* **2016**, *16*, 15–21. [CrossRef]
11. Lee, J.-H.; Cho, B.; Choi, E. Flexural capacity of fiber reinforced concrete with a consideration of concrete strength and fiber content. *Constr. Build. Mater.* **2017**, *138*, 222–231. [CrossRef]
12. Köksal, F.; Altun, F.; Yig˘it, I.; S¸ahin, Y. Combined effect of silica fume and steel fiber on the mechanical properties of high strength concretes. *Constr. Build. Mater.* **2008**, *22*, 1874–1880. [CrossRef]
13. Yoo, D.-Y.; Yoon, Y.-S.; Banthia, N. Predicting the post-cracking behavior of normal- and high-strength steel-fiber-reinforced concrete beams. *Constr. Build. Mater.* **2015**, *93*, 477–485. [CrossRef]
14. Jang, S.-J.; Yun, H.-D. Combined effects of steel fiber and coarse aggregate size on the compressive and flexural toughness of high-strength concrete. *Compos. Struct.* **2018**, *185*, 203–211. [CrossRef]
15. Nita, S. Machine Learning Techniques Used in Big Data. *Sci. Bull. Nav. Acad.* **2016**, *19*, 466–471. [CrossRef]
16. Behnood, A.; Golafshani, E.M. Machine learning study of the mechanical properties of concretes containing waste foundry sand. *Constr. Build. Mater.* **2020**, *243*, 118152. [CrossRef]
17. Young, B.A.; Hall, A.; Pilon, L.; Gupta, P.; Sant, G. Can the compressive strength of concrete be estimated from knowledge of the mixture proportions? New insights from statistical analysis and machine learning methods. *Cem. Concr. Res.* **2018**, *115*, 379–388. [CrossRef]
18. Akande, K.O.; Owolabi, T.O.; Twaha, S.; Olatunji, S.O. Performance Comparison of SVM and ANN in Predicting Compressive Strength of Concrete. *IOSR J. Comput. Eng.* **2014**, *16*, 88–94. [CrossRef]
19. Chou, J.-S.; Tsai, C.-F.; Pham, A.-D.; Lu, Y.-H. Machine learning in concrete strength simulations: Multi-nation data analytics. *Constr. Build. Mater.* **2014**, *73*, 771–780. [CrossRef]
20. Duan, J.; Asteris, P.G.; Nguyen, H.; Bui, X.-N.; Moayedi, H. A novel artificial intelligence technique to predict compressive strength of recycled aggregate concrete using ICA-XGBoost model. *Eng. Comput.* **2020**, *37*, 3329–3346. [CrossRef]
21. Gupta, S.M. Support Vector Machines based Modelling of Concrete Strength. *World Acad. Sci. Eng. Technol.* **2007**, *36*, 305–311.
22. Chou, J.-S.; Pham, A.-D. Enhanced artificial intelligence for ensemble approach to predicting high performance concrete compressive strength. *Constr. Build. Mater.* **2013**, *49*, 554–563. [CrossRef]
23. Deepa, C.; Sathiyakumari, K.; Sudha, V. Prediction of the Compressive Strength of High Performance Concrete Mix using Tree Based Modeling. *Int. J. Comput. Appl.* **2010**, *6*, 18–24. [CrossRef]
24. Erdal, H.I. Two-level and hybrid ensembles of decision trees for high performance concrete compressive strength prediction. *Eng. Appl. Artif. Intell.* **2013**, *26*, 1689–1697. [CrossRef]

25. Öztas¸, A.; Pala, M.; Özbay, E.; Kanca, E.; Çaglar, N.; Bhatti, M.A. Predicting the compressive strength and slump of high strength˘ concrete using neural network. *Constr. Build. Mater.* **2006**, *20*, 769–775. [CrossRef]
26. Sarıdemir, M. Predicting the compressive strength of mortars containing metakaolin by artificial neural networks and fuzzy logic. *Adv. Eng. Softw.* **2009**, *40*, 920–927. [CrossRef]
27. Anwar, M.K.; Shah, S.A.R.; Azab, M.; Shah, I.; Chauhan, M.K.S.; Iqbal, F. Structural Performance of GFRP Bars Based HighStrength RC Columns: An Application of Advanced Decision-Making Mechanism for Experimental Profile Data. *Buildings* **2022**, *12*, 611. [CrossRef]
28. Abbass, W.; Khan, M.I.; Mourad, S. Evaluation of mechanical properties of steel fiber reinforced concrete with different strengths of concrete. *Constr. Build. Mater.* **2018**, *168*, 556–569. [CrossRef]
29. Reddy, V.M.; Rao, M.V.S. Effect of w/c ratio on workability and mechanical properties of high strength Self Compacting Concrete
(M70 grade). *IOSR J. Mech. Civ. Eng.* **2014**, *11*, 15–21. [CrossRef]
30. Nili, M.; Afroughsabet, V. Combined effect of silica fume and steel fibers on the impact resistance and mechanical properties of concrete. *Int. J. Impact Eng.* **2010**, *37*, 879–886. [CrossRef]
31. Açikgenç, M.; Alyamaç, K.E.; Ulucan, Z.Ç. Relation between Splitting Tensile and Flexural Strengths of Steel FiberReinforced Concrete Relation between Splitting Tensile and Flexural Strengths. 2015, no. August 2016. Available online: https://www.researchgate.net/publication/278022867_Relation_between_Splitting_Tensile_and_Flexural_Strengths_of_Steel_ Fiber-Reinforced_Concrete (accessed on 9 June 2022).
32. Li, W. Analysis of the Influence of Water-cement Ratio on Concrete Strength. *E3S Web Conf.* **2021**, *283*, 01016. [CrossRef]
33. Shah, M.S.A.; Noor, N.M.; Kueh, A.B.H.; Tamin, M.N. Effects of water-cement ratio and notches to the flexural strength of concrete. *IOP Conf. Ser. Mater. Sci. Eng.* **2020**, *849*, 1–10. [CrossRef]
34. Lee, C.J.; Lange, D.A.; Lee, J.Y.; Shin, S.W. Effects of Fiber Volume Fraction and Water/Cement Ratio on Toughness Development of Steel Fiber Reinforced Concrete. *J. Korea Inst. Build. Constr.* **2013**, *13*, 20–28. [CrossRef]
35. Balanji, E.K.Z. Effect Of Water/Cement Ratio and Fiber Content on Mechanical Properties and Impact Resistance of Steel Fiber Reinforced Concrete Mixtures. Master's Thesis, Ege University, Bornova, Turkey. [CrossRef]
36. Kim, J.J.; Kim, D.J.; Kang, S.T.; Lee, J.H. Influence of sand to coarse aggregate ratio on the interfacial bond strength of steel fibers in concrete for nuclear power plant. *Nucl. Eng. Des.* **2012**, *252*, 1–10. [CrossRef]
37. Chitlange, M.R.; Pajgade, P.S. Strength appraisal of artificial sand as fine aggregate in SFRC. *J. Eng. Appl. Sci.* **2010**, *5*, 34–38.
38. Dashrath, K.B.; Anil, N.M.; Wakchaure, M.R.; Kulkarni, V.P.; Nagar, A. Effect of aggregate types on flexural strength of concrete.
Int. J. Sci. Eng. Technol. **2014**, *909*, 906–909.
39. El-Ariss, B. Effect of reducing coarse aggregates on concrete strength. *Constr. Build. Mater.* **2006**, *20*, 149–157. [CrossRef]
40. Sunarso, M.; Soeprapto, G.; Murdono, F. Effect of sand-to-aggregate volume ratio on mechanical properties concrete. *IABSE-JSCE*
Jt. Conf. Adv. Bridg. Eng. **2020**, *59*, 1–16.
41. Sunarso, M.; Soeprapto, G.; Murdono, F. Effect of sand to aggregate ratio and dosage of admixture on high strength concrete properties. In Proceedings of the AIP Conference Proceedings, Palembang, Indonesia, 14–17 August 2017; Volume 1903. [CrossRef]
42. Khan, M.; Ali, M. Effect of super plasticizer on the properties of medium strength concrete prepared with coconut fiber. *Constr. Build. Mater.* **2018**, *182*, 703–715. [CrossRef]

43. Aruntas¸, H.Y.; Cemalgil, S.; S¸ims¸ek, O.; Durmus¸, G.; Erdal, M. Effects of super plasticizer and curing conditions on properties of concrete with and without fiber. *Mater. Lett.* **2008**, *62*, 3441–3443. [CrossRef]
44. Nili, M.; Afroughsabet, V. Property assessment of steel–fibre reinforced concrete made with silica fume. *Constr. Build. Mater.* **2012**, *28*, 664–669. [CrossRef]
45. Shafieyzadeh, M. Prediction of Flexural Strength of Concretes Containing Silica Fume and Styrene-Butadiene Rubber (SBR) with an Empirical Model. *J. Inst. Eng. Ser. A* **2015**, *96*, 349–355. [CrossRef]
46. Shmlls, M.; Bozsaky, D.; Horváth, T. Compressive, flexural and splitting strength of fly ash and silica fume concrete. *Pollack Period.* **2022**, *17*, 50–55. [CrossRef]
47. Saravana, R.M.K.; Sumathi, A. Effect of fly ash in fiber reinforced concrete composites. *Jordan J. Civ. Eng.* **2017**, *11*, 30–39.
48. Challoob, M.A.; Srivastava, V.; Materials, A. Effect of Fly Ash and Steel Fibre on Portland Pozzolana Cement Concrete. *Int. J. Eng. Trends Technol.* **2013**, *5*, 144–147.
49. Saha, A.K. Effect of class F fly ash on the durability properties of concrete. *Sustain. Environ. Res.* **2018**, *28*, 25–31. [CrossRef] 90. Nath, P.; Sarker, P. Effect of Fly Ash on the Durability Properties of High Strength Concrete. *Procedia Eng.* **2011**, *14*, 1149–1156. [CrossRef]